Supplementary material

$Ca(OH)_2$-mediated activation of peroxymonosulfate for the degradation of bisphenol S

Leliang Wu[a], Yiting Lin[a], Yimin Zhang[a], Peng Wang[a], Mingjun Ding[a], Minghua Nie* [a] [b] and Caixia Yan* [a]

[a] School of Geography and Environment, Key Laboratory of Poyang Lake Wetland and Watershed Research, Ministry of Education, Jiangxi Normal University, Nanchang 330022, China

[b] Key Laboratory of Eco-geochemistry, Ministry of Natural Resource, Beijing 100037, China

* Corresponding author email: mhnie@jxnu.edu.cn (M. Nie); wysycx@foxmail.com (C. Yan)

Table S1. Basic physical and chemical characteristics of different water matrices and removal of ACE in these matrices.

Water matrixes	Degradation of BPS (%)	Cl^- ($mg \cdot L^{-1}$)	F^- ($mg \cdot L^{-1}$)	NO_2^- ($mg \cdot L^{-1}$)	SO_4^{2-} ($mg \cdot L^{-1}$)	NO_3^- ($mg \cdot L^{-1}$)	k_{obs} (min^{-1})	*Half-life*[a] (min)	R^2
Ultrapure water	100	n.d.[b]	n.d.	n.d.	n.d.	n.d.	0.2010	4.595195	0.995
River water	85.03	16.4728	1.3848	n.d.	33.4097	14.1677	0.0829	6.366535	0.997
Lake water	81.47	13.3090	0.7952	n.d.	15.7176	6.2020	0.0729	6.623628	0.997
Domestic water	77.94	15.1818	0.8712	0.3201	15.7535	8.5110	0.0626	6.928274	9.996

[a] Calculated from the pseudo-first order kinetics law where 1 / (2t) = ln2 / k_{obs}.

[b] n.d.: not detected

Table S2. Detail information of HPLC analysis.

Compounds	Mobile phase and proportion (%)	Flow rate ($mL•min^{-1}$)	Detector	Detection wavelength (nm)	Temperature of column incubator (°C)	Injection volume (μl)
BPA	Water: Methanol 20: 80	0.2	DAD	220	40	2
BPS	Water: Methanol 40: 60	0.2	DAD	258	40	2
FFA	Methanol: Trifluoroacetic acid (0.5‰) 30: 70	0.2	DAD	214	40	2
TAP	Methanol: Trifluoroacetic acid (0.5‰) 25: 75	0.3	FLD	λ_{ex} = 224 λ_{em} = 290	40	2
NOF	Methanol: Trifluoroacetic acid (0.5‰) 25: 75	0.3	FLD	λ_{ex} = 278 λ_{em} = 445	40	2
ENR	Methanol: Trifluoroacetic acid (0.5‰) 28: 72	0.3	FLD	λ_{ex} = 280 λ_{em} = 450	40	2
LOM	Methanol: Trifluoroacetic acid (0.5‰) 30: 70	0.3	FLD	λ_{ex} = 338 λ_{em} = 425	40	2

Table S3. Removal of BPS by $Ca(OH)_2$/PMS system in the presence of various substances. Experiment conditions: $[BPS]_0$ =20 μm, $[PMS]_0$ = 1.5 mM, $[Ca(OH)_2]_0$ = 1 mM, $[substances]_0$ = 0-10 mM, $[HA]_0$ = 0-50 mg•L^{-1}.

Coexisting	Concentrations	Removal of	k_{obs}	R^2	Initial-final
No addition	-	100%	2.01×10^{-2}	0.995	9.83-7.03
Cl^-	1 mM	98.01	1.57×10^{-2}	0.963	10.77-9.17
	5 mM	100	2.53×10^{-2}	0.900	10.82-9.09
	10 mM	100	2.78×10^{-2}	0.777	10.89-8.97
HCO_3^-	1 mM	89.71	9.70×10^{-3}	0.999	10.16-9.01
	5 mM	67.57	4.80×10^{-3}	0.991	9.64-9.02
	10 mM	63.82	4.30×10^{-3}	0.981	9.5-9.16
NO_3^-	1 mM	100.00	2.03×10^{-2}	0.993	9.86-7.61
	5 mM	100.00	1.95×10^{-2}	0.995	10.07-7.80
	10 mM	99.35	2.09×10^{-2}	0.987	10.16-7.88
SO_4^{2-}	1 mM	99.23	2.04×10^{-2}	0.994	9.9-7.75
	5 mM	100.00	1.94×10^{-2}	0.991	10.52-8.33
	10 mM	99.40	2.09×10^{-2}	0.974	10.28-8.19
HA	5 mg•L^{-1}	98.62	1.79×10^{-2}	0.992	9.93-7.56
	20 mg•L^{-1}	96.83	1.49×10^{-2}	0.996	9.74-7.55
	50 mg•L^{-1}	96.31	1.42×10^{-2}	0.993	10.4-7.70

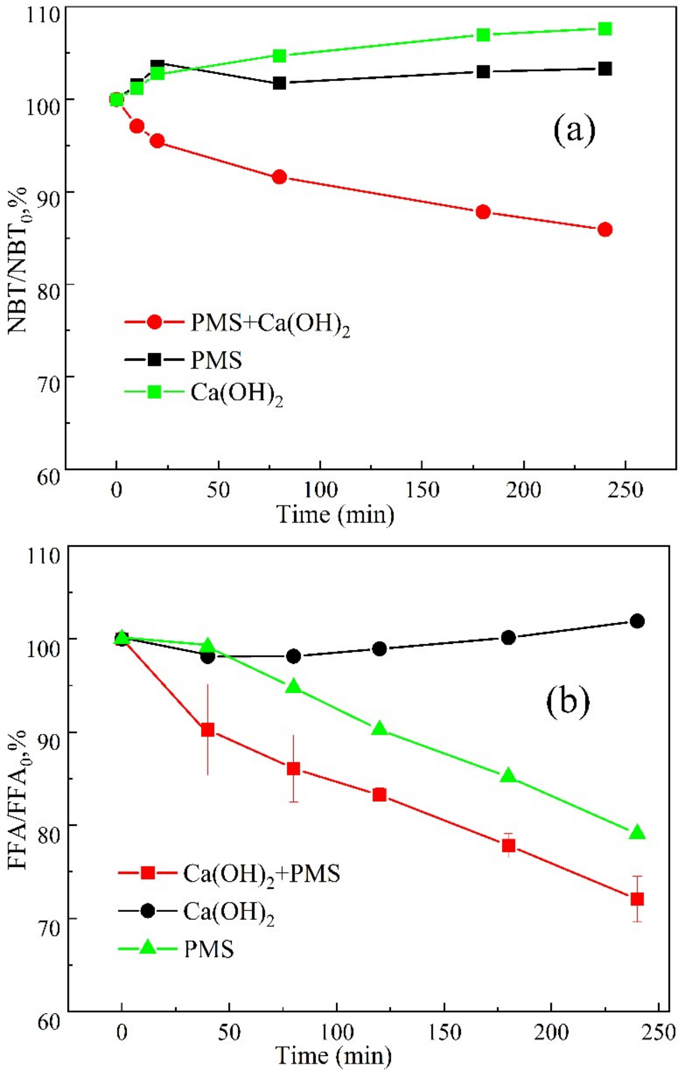

Fig. S1. Degradation of NBT (a), and FFA (b)in the $Ca(OH)_2$/PMS system, $[Ca(OH)_2]_0$ = 1 mM, $[PMS]_0$ = 1.5 mM, $[NBT]_0$ = $[FFA]_0$ = 20 μM.

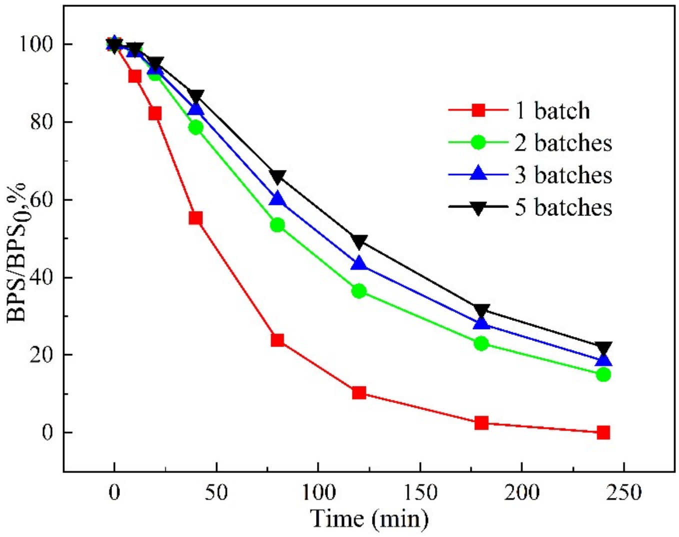

Fig. S2 Effect of PMS adding modes on the degradation of PMS. $[Ca(OH)_2]_0$ = 1 mM, $[PMS]_0$ = 1.5 mM, $[BPS]_0$ = 20 μM.

Table R1. Removal of BPS by different oxidation methods

Oxidation methods	BPS dosages	Experimental conditions	Reaction time	BPS degradation rate	Degradation mechanism	References
α-Fe_2O_3 nanosheets, visible light	80 μM	0.2 g•L^{-1} catalyst, 0.2 g•L^{-1} H_2O_2, pH=5.6 ± 0.2, 25°C	160 min	91%	h^+ and •OH	Shao et al., 2017[1]
Heat, PS	25 μM	0.5 mM PS, pH=7.0, 60°C	180 min	91%	$SO_4^{\bullet-}$	Wang et al., 2017[2]
Spinel sulfide, PMS	10 μM	0.01 g•L^{-1} catalyst, 0.1 mM PS, 25°C	30 min	100%	$SO_4^{\bullet-}$	Xu et al., 2018[3]
Ferrate	5 μM	0.05 mM Ferrate, 25°C	10 min	90%	$HFeO_4^-$	Yang et al., 2019[4]
visible light, BIOI/B_4C, PMS	20 μM	100 mg•L^{-1} BIOI/B_4C, 0.05 mM PMS, pH = 7.0 ± 0.5, 25°C	45 min	90.4%	h^+, •OH, $SO_4^{\bullet-}$, $O_2^{\bullet-}$	Lv et al., 2021[5]
$Ca(OH)_2$, PMS	20 μM	1.5 mM PMS, 1 mM $Ca(OH)_2$, 25°C	240 min	100%	$O_2^{\bullet-}$ and $^1O_2$	Present study

Table R2 The structures and basic properties of BPS.

Molecular structure	Molecular formula	Molecular weight	Denisity (g/cm^3)	*pKa*	Melting point (°C)
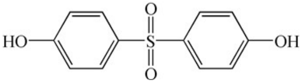	$C_{12}H_{10}O_4S$	250.2	1.433	8.2	240

Table R3. Removal of BPS by $Ca(OH)_2$/PMS system in the presence of various substances. Experiment conditions: $[BPS]_0$ =20 μm, $[PMS]_0$ = 0-3 mM, $[Ca(OH)_2]_0$ = 0-2 mM, $[HA]_0$ = 0-50 mg•L^{-1}.

Coexisting substance	Concentration	Removal of BPS(%)	k_{obs} (min^{-1})	R^2	Initial-final pH
different systems	only PMS	3.57	1.17×10^{-4}	0.742	3.96-3.38
	only $Ca(OH)_2$	1.05	1.74×10^{-5}	0.033	11.12-10.97
	PMS+$Ca(OH)_2$	100	2.01×10^{-2}	0.995	9.69-8.20
	PS+$Ca(OH)_2$	0	6.64×10^{-5}	0.346	-
	H_2O_2+$Ca(OH)_2$	0	9.88×10^{-5}	0.723	-
initial $Ca(OH)_2$	0.00 mM	1.05	1.17×10^{-4}	0.742	3.45-3.26
	0.25 mM	3.70	1.38×10^{-4}	0.855	3.66-3.61
	0.50 mM	6.42	1.92×10^{-4}	0.652	8.03-5.28
	0.75 mM	89.32	1.01×10^{-2}	0.988	9.24-6.06
	1.00 mM	100	2.01×10^{-2}	0.995	9.69-8.20
	1.50 mM	82.17	7.53×10^{-3}	0.953	10.89-10.97
	2.00 mM	38.16	1.94×10^{-3}	0.852	10.96-10.94
initial PMS	0.00 mM	1.05	1.74×10^{-5}	0.032	11.12-10.97
	0.50 mM	12.79	5.40×10^{-4}	0.934	10.92-10.79
	1.00 mM	61.23	4.09×10^{-3}	0.978	10.41-10.13
	1.25 mM	88.03	9.27×10^{-3}	0.986	10.02-9.31
	1.50 mM	100	2.01×10^{-2}	0.995	9.69-8.20
	1.75 mM	98.21	1.76×10^{-2}	0.995	9.31-8.59
	2.00 mM	98.39	1.80×10^{-2}	0.993	9.14-8.10
	3.00 mM	77.63	6.87×10^{-3}	0.928	7.65-7.50
initial BPS	10 μM	98.74	1.79×10^{-2}	0.986	9.71-8.70
	20 μM	100.00	2.01×10^{-2}	0.995	9.69-8.20
	40 μM	91.94	1.14×10^{-2}	0.971	10.36-7.85
	60 μM	84.63	8.60×10^{-3}	0.898	9.71-7.23
	80 μM	77.08	6.60×10^{-3}	0.863	9.57-7.21
temperature	4°C	43.12	2.40×10^{-3}	0.997	10.44-9.44
	25°C	100	2.01×10^{-2}	0.995	9.69-8.20
	40°C	100	2.11×10^{-2}	0.994	9.33-7.24
	50°C	100	5.92×10^{-2}	0.972	9.64-7.43

References:

1 X. Wang, J. Ma, H., Z. Wang, R. Guo, and X. Hu, Aqueous phototrans-formation of bisphenol S: The competitive radical-attack pathway to p-hydroxybenzene-sulfonic acid. *Water Sci. Technol.*, 2014, 70(3), 540-547.

2 P. Shao, Z. Ren, J. Tian, S. Gao, X. Luo, W. Shi and F. Cui, Silica hydrogel-mediated dissolution-recrystallization strategy for synthesis of ultrathin a-Fe_2O_3 nano-sheets with highly exposed (110) facets: A superior photocatalyst for degradation of bisphenol S. *Chem Eng. J.*, 2017, 323, 64-73.

3 Q. Wang, X. Lu, Y. Cao, J. Ma, J. Jiang, X. Bai and T. Hu, Degradation of Bisphenol S by heat activated persulfate: Kinetics study, transformation pathways and influences of co-existing chemicals. *Chem Eng. J.*, 2017, 328, 236-245.

4 H. Xu, D. Wang, J. Ma, T. Zhang, X. Lu, and Z. Chen, A superior active and stable spinel sulfide for catalytic peroxymonosulfate oxidation of bisphenol S, *Appl. Catal., B*, 2018, 238, 557-567.

5 T. Yang, L. Wang, Y. Liu, Z. Huang, H. He, X. Wang, J. Jiang. D. Gao and J. Ma, Comparative study on ferrate oxidation of BPS and BPAF: Kinetics, reaction mechanism, and the improvement on their biodegradability, *Water Res*, 2019, **148**, 115-125.

6 Y. Lv, Y. Liu, J. Wei, M. Li, D. Xu and B. Lai, Bisphenol S degradation by visible light assisted peroxymonosulfate process based on BiOI/B_4C photocatalysts with Z-scheme heterojunction, *Chem Eng. J.*, 2021, 417, 129188.